Effect of Molecular Weight on the Surface Morphology, Molecular Reorientation, and Liquid Crystal Alignment Properties of Rubbed Polystyrene Films

Seung Woo Lee, Jinhwan Yoon, Hak Chul Kim, Byeongdu Lee, Taihyun Chang, and Moonhor Ree*

Department of Chemistry, Division of Molecular and Life Sciences, BK21 Program, Center for Integrated Molecular Systems, and Polymer Research Institute, Pohang University of Science & Technology, San 31, Hyoja-dong, Nam-gu, Pohang 790-784, Republic of Korea

Received August 25, 2003; Revised Manuscript Received October 20, 2003

ABSTRACT: The molecular reorientations and surface morphologies of rubbed films formed from atactic polystyrene (PS) samples with various molecular weights $\overline{M}_w$ (weight-average molecular weight) in the range 2700−83 000 and narrow polydispersity were investigated in detail by atomic force microscopy, optical retardation analysis, and linearly polarized infrared spectroscopy. We have first discovered previously unknown surface topography features in rubbed films of PS with >9800 $\overline{M}_w$: submicroscale groovelike meandering structures composed of fine groovelike pebbles in tens of nanometers are present, oriented perpendicular to the rubbing direction. The unusual surface morphology is a significant departure from the surface topographies observed so far for rubbed PS and other polymer films, for which grooves are usually only found parallel to the rubbing direction. These surface morphology variations might be due to the different deformation responses of the different molecular weight PS films to the shear forces caused by contact of fibers with the film surfaces during the rubbing process. On all the rubbed PS films, the vinyl main chains, however, were preferentially reoriented along the rubbing direction, and the planes of the phenyl side groups were preferentially reoriented perpendicular to the rubbing direction with para directions that were positioned nearly normal to the film plane. Nematic liquid crystal (LC) molecules were found to always align on the rubbed PS surfaces along the orientation direction of the submicroscale grooves generated by rubbing. However, the anchoring energies of the LC alignments were very low depending on the molecular weight of the sample, and these LC alignments all had limited stability. We conclude that the alignment of LCs with only weak molecular interactions with rubbed PS film surfaces is governed by their interactions with the submicroscale grooves in cooperation with one of the two other important interactions—those with the reoriented main chain segments and those with the reoriented side groups.

Introduction

Organic polymer thin films are widely used in the liquid crystal (LC) flat-panel display industry as alignment layers to induce the uniform, unidirectional alignment of liquid crystal (LC) molecules, which is critical to the optical and electrical performance of industrial LC flat-panel display devices.[1] The rubbing of polymer alignment layers with a rayon velvet fabric is the only treatment of polymer film alignment layer surfaces currently adopted in the LC display industry for the mass production of flat-panel LC display devices; this method offers both simplicity and control of LC alignment with regard to both the LC anchoring energy and the pretilt angle.[1] Much effort has been devoted to the development of alignment layer polymers and to understanding the LC alignment mechanism of rubbed polymer surfaces.[1−10]

Of the LC alignment layer polymers reported so far, rubbed films of atactic polystyrene (PS) were the first material reported to induce LC alignment perpendicular to the rubbing direction with zero pretilt,[5] which is very different than the LC alignment observed for the polyimide (PI) films currently used in the LC display industry (i.e., parallel to the rubbing direction).[1−4] Infrared (IR) dichroic spectroscopy and optical retardation studies found that the PS main chains on a rubbed PS surface are reoriented along the rubbing direction.[5−7] Near-edge X-ray absorption fine structure (NEXAFS) studies found that the phenyl side groups of PS are oriented by rubbing such that their planes are perpendicular to the rubbing direction with para directions that are nearly normal to the film plane.[9] Rubbed PS film surfaces have also been examined by atomic force microscopy (AFM).[7,8] From these results it has been concluded that the perpendicular LC alignment on rubbed PS films is induced by the favorable anisotropic interactions of LCs with the perpendicularly reoriented phenyl side groups, which override the interactions of the LCs with the parallel reoriented vinyl main chains and with the microgrooves developed along the rubbing direction. Thus, the alignment of LCs on rubbed PS films has widely been cited as a clue that the microgrooves generated by the rubbing process are not necessarily required to create a preferential alignment of LCs on an alignment layer surface.

However, the above statements as to the reorientations of the polymer main chains and the phenyl side groups on rubbed PS film surfaces were derived qualitatively from limited and independent measurements, as is briefly reviewed in the following. The reorientation of PS main chains has only been estimated qualitatively from either the dichroic ratio of the methylene asym-

* To whom all correspondence should be addressed: Tel +82-54-279-2120; Fax +82-54-279-399; e-mail ree@postech.edu.

10.1021/ma035258z CCC: $25.00
Published on Web 11/26/2003

metric stretching vibrations obtained from spectra measured parallel and perpendicular to the rubbing direction by IR spectroscopy[5] or from optical retardation measurements.[6,7] NEXAFS studies were conducted on rubbed PS films, but only information about the reorientations of the phenyl rings was obtained.[9] The zero pretilt behavior of LCs on the rubbed PS films was also discussed, but no clear picture of the zero pretilt phenomenon was obtained from these NEXAFS results.[9] Rubbed PS film surfaces have also been examined by AFM,[7] but the conclusions were only qualitative; in fact, the AFM instruments used in these studies conducted in the early 1990s have been known to have a very poor image resolution. A high-resolution AFM study of rubbed PS films was additionally reported in 1998 but did not show any LC alignment property of the rubbed films.[8] Detailed information on the surface morphology of rubbed PS films is still essential for understanding the mechanism of LC alignment on these surfaces. Moreover, no detailed information on the molecular weight and polydispersity of the PS materials used in the earlier studies is available;[5−7] the PS materials used in those studies were received as commercial product grades from various polymer manufacturers. If the exact mechanism behind the unusual LC alignment with zero pretilt is to be understood, the rubbing-induced reorientations of all PS chain segments and the rubbed film surface morphology must be quantitatively and comprehensively investigated.

To examine quantitatively the surface morphology, molecular reorientation, and LC alignment properties of rubbed PS films, we chose in the present study to examine a series of atactic PS materials with weight-average molecular weights $\overline{M_w}$ in the range 2700−83 000 and narrow polydispersity (PDI) that were synthesized by anionic polymerization. The orientational distributions of the main chains and the side groups in the PS films were quantitatively investigated before and after rubbing using linearly polarized FTIR spectroscopy and optical retardation analysis. We also examined the films' surface topographies using high spatial resolution AFM. The alignment behaviors of LC molecules on the surfaces were examined for rubbed PS films coated with a Merck nematic LC (MLK-6424). Further, antiparallel and 90°-twisted cells were assembled from the rubbed films and injected with LC, and the pretilt angles and the anchoring energies of the LC molecules were measured. We discovered grooves in the rubbed film surfaces with shapes and directors that are dependent upon the molecular weight and found that the grooves contribute significantly to the observed LC alignments. The observed LC alignments are discussed by taking into account the interactions of the LC molecules with the grooves and with the reoriented polymer segments.

Experimental Section

A series of atactic PS materials were purchased from Polysciences Co. (Los Angeles, CA) with the following molecular weights and polydispersities, listed as $\overline{M_w}$ (PDI): 2700 (1.10), 5200 (1.03), 9800 (1.02), 19 200 (1.01), 37 000 (1.01), 63 000 (1.01), 68 000 (1.01), 83 000 (1.02). Tetrahydrofuran (THF) was purchased from Aldrich Chemical Co., and a nematic LC [MLK-6424: n_e (extraordinary refractive index) = 1.5697 and n_o (ordinary refractive index) = 1.4769] was obtained from Merck Co. All materials were used without further purification.

A solution of each PS sample was prepared in THF (2 wt % solid). Each PS solution was spin-coated onto calcium fluoride windows for the FTIR spectra, onto gold-coated silicon wafers for the AFM measurements, and onto indium tin oxide glass substrates for the optical retardation measurements and LC cell assembly. The films were dried at 120 °C for 12 h. The resulting films were measured to have a thickness of around 200 nm, using a spectroscopic ellipsometer (J.A. Woollam Co., model VASE). The PS films coated onto substrates were rubbed using a laboratory rubbing machine (Wande Co.) with a roller covered by a rayon velvet fabric (Yoshikawa Co., model YA-20-R). The rubbing density (L/l) was varied by changing the cumulative rubbing time for a constant rubbing depth of 0.15 mm: $L/l = N[(2\pi rn/60v) - 1]$, where L is the total length of the rubbing cloth which contacts a certain point of the polymer film (mm), l is the contact length of circumference of rubbing roller (mm), N is the cumulative number of rubbings, n and r are the speed (rpm) and the radius (cm) of rubbing roller (rpm), respectively, and v is the velocity (cm/s) of the substrate stage.[3,10,11]

Some of the rubbed PS films on glass substrates were cut into 2.5 cm × 2.5 cm pieces and then used for assembling two different LC cells as follows. First, paired pieces from each glass substrate were assembled together orthogonally with respect to the rubbing direction by using silica balls of 4.0 μm diameter as spacers, injected with the Merck LC, and then sealed with an epoxy glue, giving 90°-twisted nematic LC cells (TN cells). Second, paired pieces cut from each glass substrate were assembled together antiparallel with respect to the rubbing direction by using 50 μm thick spacers, injected with the Merck LC, and then sealed with epoxy glue, giving antiparallel nematic LC cells. These LC cells were then aged at room temperature for 3−5 h in order to remove any flow-induced memory possibly induced by the LC injection process; using an optical microscope and a cross-polarized optic system with a He−Ne laser (632.8 nm wavelength), the aged LC cells were inspected not to have any flow-induced memory, regardless of the direction of LC injection into the cell with respect to the rubbing direction. In addition, a solution of the Merck LC in ethyl ether (10 wt % LC) was directly spin-coated onto some of the rubbed PS films at 4500 rpm for 60 s, which were then dried at room temperature for 3 h; the typical thickness of the coated LC layers was around 300 nm, as measured using the spectroscopic ellipsometer.

The glass transition temperature (T_g) of each PS sample was measured in the range −10 to 200 °C using a differential scanning calorimeter (DSC) (model DSC 220CU, Seiko, Japan). Each PS sample was preheated to 200 °C and soaked at that temperature for 10 min in order to remove any thermal history, then cooled at 10.0 °C/min to −10 °C, and once more heated at 10.0 °C/min up to 200 °C. T_g was determined as the onset temperature of the glass transition in the thermogram obtained in the second heating run. During the measurements, dry nitrogen gas was used for purging; a flow rate of 80 cm^3/min and a ramping rate of 10.0 °C/min were employed. In each run, a sample of about 5 mg was used.

Optical phase retardations were measured using an optical setup described elsewhere;[10] the laser beam was incident normal to the surface of the film, and the transmitted light intensity was monitored as a function of the angle of rotation of the film sample with respect to the surface normal. Polarized FTIR spectroscopic measurements in transmission and reflection modes were carried out on a Bomem DA8 FTIR spectrometer equipped with a polarizer (single diamond polarizer, Harrick Scientific). For all transmission FTIR spectra, the film planes of the samples were installed perpendicular to the incident beam direction. IR spectra were recorded at 4 cm^{-1} resolution with a liquid nitrogen cooled mercury cadmium telluride detector under vacuum as a function of the angle of rotation of the polarizer, and interferograms were accumulated 256 times. External reflection IR spectra were measured with 4 cm^{-1} resolution at an incidence angle of 82°, and interferograms were accumulated 512 times. AFM surface images were obtained using a tapping mode atomic force microscope (Digital Instruments, model Multimode AFM Nanoscope IIIa). An ultralever cantilever (with a 26 N/m spring constant and 268 kHz resonance frequency) was used for scanning.

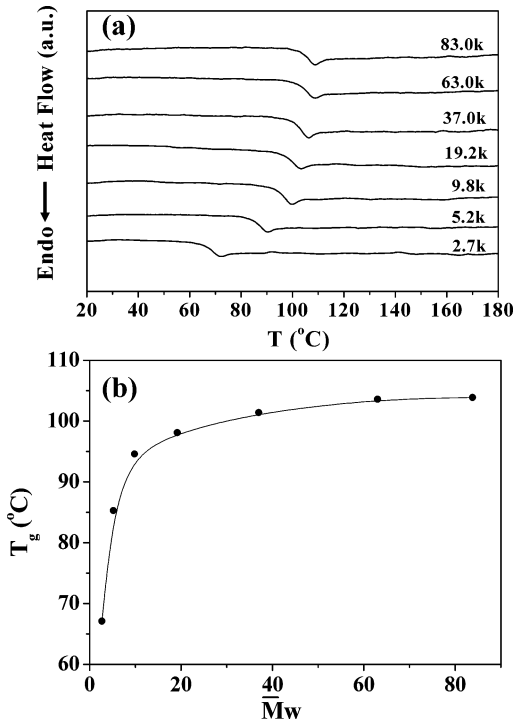

Figure 1. (a) DSC thermograms for PS polymers with various molecular weights. (b) Variation of the T_g of PS with weight-average molecular weight $\overline{M_w}$. All the DSC measurements were conducted at a heating rate of 10.0 °C/min under nitrogen gas flow.

For the antiparallel LC cells, the polar anchoring energies and the pretilt angles were measured using a polar anchoring energy apparatus[12] and a crystal rotation apparatus,[3,10] respectively. For the TN LC cells, the azimuthal anchoring energy was measured by using an ultraviolet−visible (UV−vis) spectrophotometer (model S-300, Scinco, Korea) equipped with two Glan-Laser prisms (one a polarizer and the other an analyzer, model PGL5015, Casix, China); the analyzer was mounted on a motorized goniometer (model SKIDS-PH, Sigma Koki, Tokyo, Japan). Each TN cell was placed between the polarizer and the analyzer. UV−vis spectra were recorded at 0.8 cm^{-1} resolution as a function of the angle of rotation of the analyzer in the range 0−180° with an interval of 1.0°. The rotation angles with minimum transmittance in the UV−vis spectra were determined from these measurements. These angles were used for determining the twist angles at which the easy axes of the upper and lower substrates of the TN cell occur.[13] From the twist angles, the azimuthal anchoring energies of the LCs on the rubbed PS film surfaces were estimated using the optical parameters of the Merck LC, according to a method reported elsewhere.[11] In addition, the cell gap was determined from the UV−vis spectra.

Results and Discussion

Glass Transitions. Figure 1 shows the DSC thermograms obtained for the PS samples and the glass transition temperatures determined from the thermograms. As can be seen in Figure 1b, the T_g of PS varies over the wide range 67−104 °C, depending upon the molecular weight; T_g rapidly increases with increasing molecular weight in the low-$\overline{M_w}$ region (<19 200 $\overline{M_w}$) and then increases more slowly with further increases in the molecular weight.

Molecular Reorientation. Figure 2 shows the variation of the optical retardation [= (in-plane birefringence) × (film thickness)] of PS (68 000 $\overline{M_w}$) films rubbed with varying rubbing density. All the rubbed films exhibit

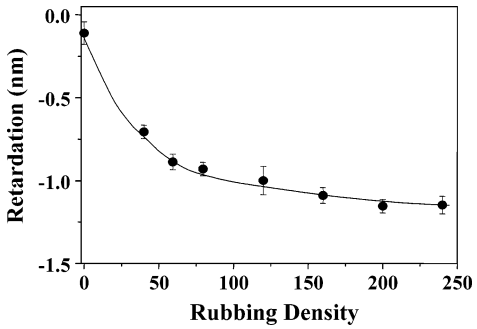

Figure 2. Variation of the optical retardation [= (in-plane birefringence) × (film thickness)] of a PS film with $\overline{M_w}$ = 68 000 rubbed with varying rubbing density.

negative retardation values. These negative retardation values are due to the negative birefringence of the PS polymer chain, which arises because the phenyl side group has a larger polarizability than the vinyl chain backbone. As can be seen in the figure, the retardation (i.e., degree of reorientation of the PS polymer chains) of the rubbed PS films rapidly decreases with rubbing density for rubbing densities up to around 80 and then more slowly decreases with further increases in the rubbing density. Taking this result into account, a rubbing density of 60 was chosen for the remaining studies of rubbed PS films, in which the films were examined by optical retardation and linearly polarized FTIR spectroscopy.

Figure 3 shows polar diagrams of the transmitted light intensities [= (in-plane birefringence) × (phase)] of the rubbed PS films, which were constructed from the optical retardation measurements as a function of the angle of rotation of the films. All the polar diagrams exhibit a maximum intensity of transmitted light along the direction 270° ↔ 90°, which is perpendicular to the rubbing direction, regardless of the molecular weight of the PS sample. In a PS chain, the favored conformation of the phenyl side group is orthogonal to the vinyl backbone. The anisotropic polar diagram results thus indicate that the rubbing of PS films preferentially reorients the phenyl side groups perpendicular to the vinyl main chains, which are themselves reoriented parallel to the rubbing direction, regardless of the molecular weight of the sample.

Figure 4a displays representative dichroic IR spectra of a PS film (68 000 $\overline{M_w}$) rubbed at a rubbing density of 60. As can be seen in the figure, the PS films exhibit quadrant C═C stretching vibrations (1602 and 1583 cm^{-1}) and semicircle C═C stretching vibrations (1492 and 1452 cm^{-1}) of the phenyl ring, as well as the asymmetric CH_2 stretching vibration (2925 cm^{-1}) and symmetric CH_2 stretching vibration (2852 cm^{-1}) of the vinyl backbone, as assigned using previously reported results.[14] The dipole transition moments of the 1602 and 1492 cm^{-1} bands are known to be oriented along the para direction of the phenyl ring, while those of the 1583 and 1452 cm^{-1} bands are oriented in the plane of the aromatic ring but perpendicular to the dipole transition moments for the 1602 and 1492 cm^{-1} bands.[14] The dipole transition moment for the asymmetric CH_2 stretching vibration is orthogonal to the dipole transition moment for the symmetric CH_2 stretching vibration, and both these dipole transition moments are oriented perpendicular to the polymer backbone.[12] All these bands are more intense when the incident IR beam is polarized perpendicular to the rubbing direction

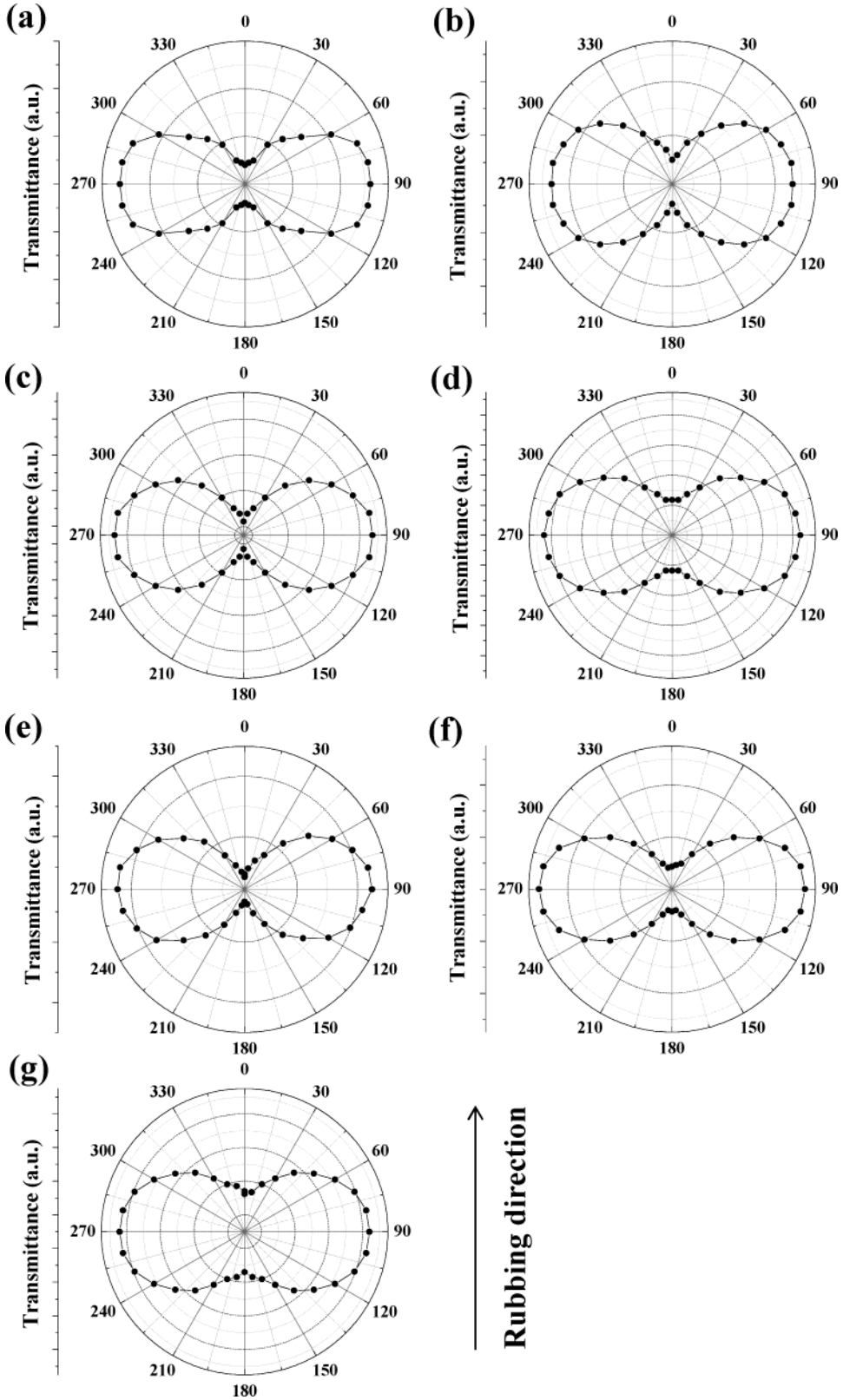

Figure 3. Polar diagram of the light transmittance [= (in-plane birefringence) × (phase)] as a function of the angle of rotation of the film constructed from the optical phase retardation measurements of PS films with varying molecular weights rubbed with a rubbing density of 60: (a) 2700 $\overline{M_w}$, (b) 5200, (c) 9800, (d) 19 200, (e) 37 000, (f) 63 000, and (g) 83 000.

(the dashed line in Figure 4a). Taking into account this anisotropic dichroic IR result and the above band assignments, we selected two representative bands (1492 and 2925 cm^{-1}) and then further monitored their peak intensity changes as a function of the angle of rotation of the film to gain information on the reorientations of the phenyl rings and the vinyl backbones. As shown in Figure 4b,c, both bands are more intense when the polarization of the incident beam is perpendicular to the rubbing direction. These IR results imply that on rubbed PS film surfaces the phenyl rings are preferentially reoriented perpendicular to the rubbing

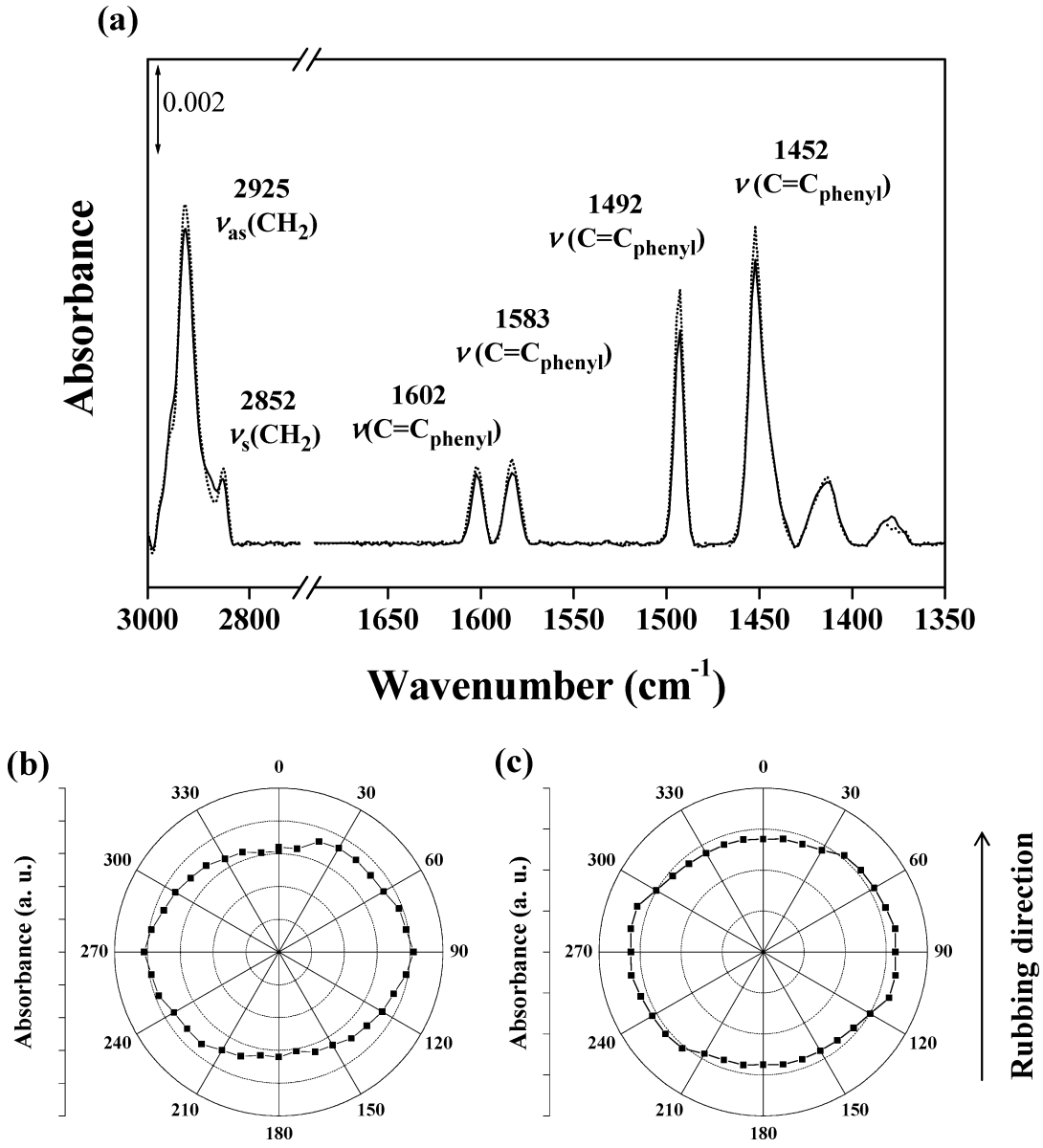

Figure 4. (a) FTIR dichroic spectra of a PS film with 68 000 $\overline{M_w}$ rubbed with a rubbing density of 60: solid and dashed lines represent the FTIR spectra with IR light polarized parallel and perpendicular to the rubbing direction, respectively. Polar diagrams of two vibrational bands selected from (a) as a function of the angle of rotation of the film, obtained using linearly polarized IR spectroscopy: (b) 1492 and (c) 2925 cm^{-1}.

direction while the polymer backbones are aligned parallel to the rubbing direction, which supports the result derived from the optical retardation measurements described above.

On the other hand, in the reflection spectrum measured with the IR light polarized parallel to the rubbing direction and propagated toward the rubbing direction, the phenyl bands at 1602 and 1492 cm^{-1} were found to be more intense than in the transmission spectrum measured with the IR light polarized parallel to the rubbing direction (see Figure 5). In contrast, the phenyl bands at 1583 and 1452 cm^{-1} were much weaker in intensity in the reflection spectrum than in the transmission spectrum (see Figure 5). These spectral results indicate that the para directions of the phenyl side groups are on average aligned nearly normal to the rubbed film surface.

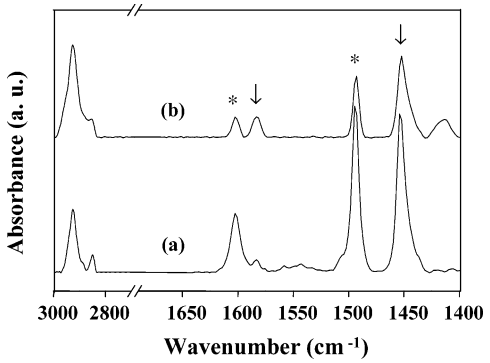

Figure 5. (a) External reflection and (b) transmission FTIR spectra of a PS film (68 000 $\overline{M_w}$) rubbed with a rubbing density of 60, which were measured with the IR light polarized parallel to the rubbing direction.

From these results for the in-plane and out-of-plane orientations of the polymer chain segments it is concluded that on rubbed PS film surfaces the vinyl main chains are reoriented parallel to the rubbing direction

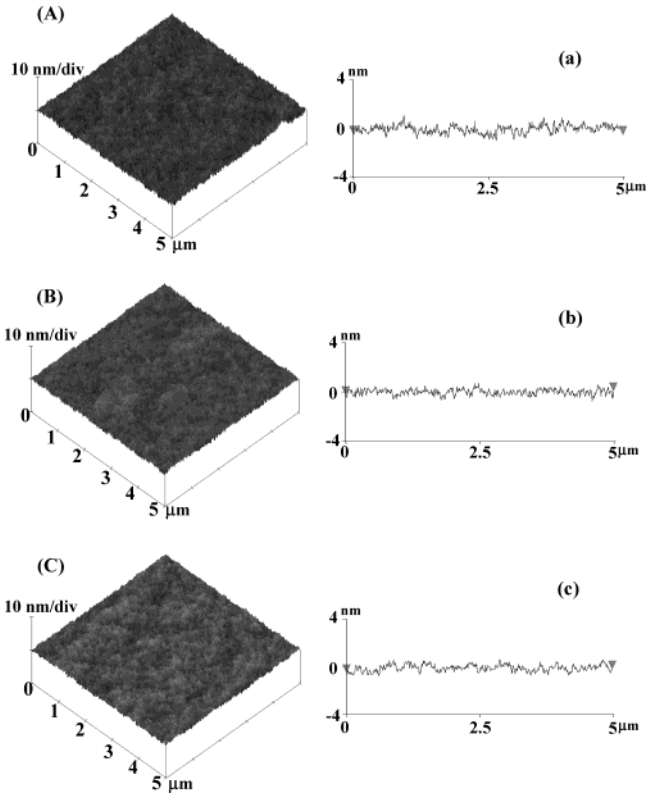

Figure 6. AFM images and surface profiles (along the lines in the AFM images) of unrubbed PS films: (A, a) 5200 $\overline{M_w}$; (B, b) 37 000; (C, c) 83 000.

while the planes of the phenyl side groups are reoriented perpendicular to the rubbing direction with para directions that are positioned nearly normal to the film plane.

Surface Morphology. Figure 6 shows some representative AFM images of unrubbed PS films. As can be seen in the figure, the surface images do not vary significantly with the molecular weight of the PS sample, and their root-mean-square (rms) surface roughnesses are in the range 0.24−0.29 nm. These surface roughnesses are relatively much smaller than that (1.4 nm rms) previously reported for PS films.[8] These AFM images indicate that the unrubbed PS films in the present study have very smooth surfaces.

All the PS films were rubbed at a rubbing density of 60, as for the optical retardation results in Figure 3, and then examined in detail by AFM. The resulting AFM images are shown in Figure 7.

Figure 7A shows an AFM image of the rubbed surface of a PS film with $\overline{M_w}$ = 2700. This rubbed film has typical scratch lines separated by approximately 2 μm, which are created on the surface by adjacent fiber pairs during the rubbing process, as is often observed for rubbed PI films.[1−4] In addition, weakly defined submicroscale grooves are discernible along the rubbing direction. Surface profiles were obtained along lines a-1 (perpendicular to the rubbing direction) and a-2 (parallel to the rubbing direction) as indicated in Figure 7A, and the results are shown in Figure 7a-1,2. These surface profiles indicate that the rms surface roughness is 3.75 nm across the submicroscale groove lines (i.e., along line a-1) and 1.18 nm along the submicroscale groove lines (i.e., along line a-2); these values are much larger than the rms surface roughness of the unrubbed PS film surface. Thus, the submicroscale grooves are made up of fine grooves (65−100 nm in size) like pebbles. A similar AFM image was obtained for rubbed PS films with 5200 $\overline{M_w}$, as shown in Figure 7B. The surface profiles in Figure 7b-1,2 indicate that the rms surface roughness of this film is 4.47 nm across the submicroscale groove lines and 1.54 nm along the submicroscale groove lines. The surface roughness of this rubbed PS film is larger than that observed for the rubbed PS film with 2700 $\overline{M_w}$.

The observed submicroscale groove morphology is somewhat different to those reported previously for rubbed PS films[7,8] and some PI films.[3e,4f] For PS films, Seo et al.[7b] found ground-beef-like surface morphology developed along the rubbing direction, which partly resembles that observed for rubbed films of a rodlike polyimide with bristles[3e] but does not resemble those reported for rubbed films of flexible polyimides.[4f] On the other hand, Wu et al.[8] observed sharp grooves with a rms surface roughness of 6.1 nm for rubbed PS, which were well developed along the rubbing direction. These surface morphology differences are perhaps attributed to the different PS characteristics such as molecular weight and distribution as well as the different rubbing conditions.

Surprisingly, rubbed PS films with 9800 $\overline{M_w}$ exhibit a previously unknown surface feature, specifically, a submicroscale meandering groovelike structure (see the left-hand section of the AFM image in Figure 7C), in addition to the submicroscale grooves composed of fine groovelike pebbles (see the right-hand section of the AFM image in Figure 7C) observed for the two PS films described above. The submicroscale meandering groovelike structures are weakly developed along the rubbing direction, and their orientation directions lie perpendicular to the rubbing direction. The surface profile in Figure 7c-1 indicates a rms surface roughness of 2.28 nm across the rubbing direction (i.e., along line c-1 in Figure 7C), which is smaller than was observed in the same direction for the two rubbed PS films discussed so far. On the other hand, the rms surface roughness along the rubbing direction (i.e., along line c-2 in Figure 7C) is 3.18 nm, which is at least 2 times larger than the above values. The surface profile in Figure 7c-2 has oscillations with a periodicity of 130−325 nm, indicating the presence of the meandering groovelike structures on the film surface.

These meandering groovelike structures are more clearly discernible in the rubbed film surfaces of PS films with 19 200 $\overline{M_w}$, as shown in the AFM image in Figure 7D. The submicroscale grooves composed of fine groovelike pebbles observed in the rubbed PS films with 2700 and 5200 $\overline{M_w}$ are not discernible in PS films with 19 200 $\overline{M_w}$. Parts d-1 and d-2 of Figure 7 show surface profiles obtained across and along the rubbing direction, i.e., along the lines d-1 and d-2 in Figure 7D, respectively. The rms surface roughnesses across and along the rubbing direction are 4.11 and 5.60 nm, respectively; these values are larger than those of the rubbed PS films of lower molecular weight (i.e., 2700−9800 $\overline{M_w}$). The surface profile oscillates with a periodicity of approximately 650 nm across the rubbing direction and with a periodicity of approximately 195 nm along the rubbing direction; the height of these profiles is approximately 14 nm. These data indicate that each meandering groovelike structure is approximately 650 nm long, 195 nm wide, and 14 nm high. Further, the oscillation pattern in Figure 7d-2 shows greater periodicity than that observed in the same direction for the

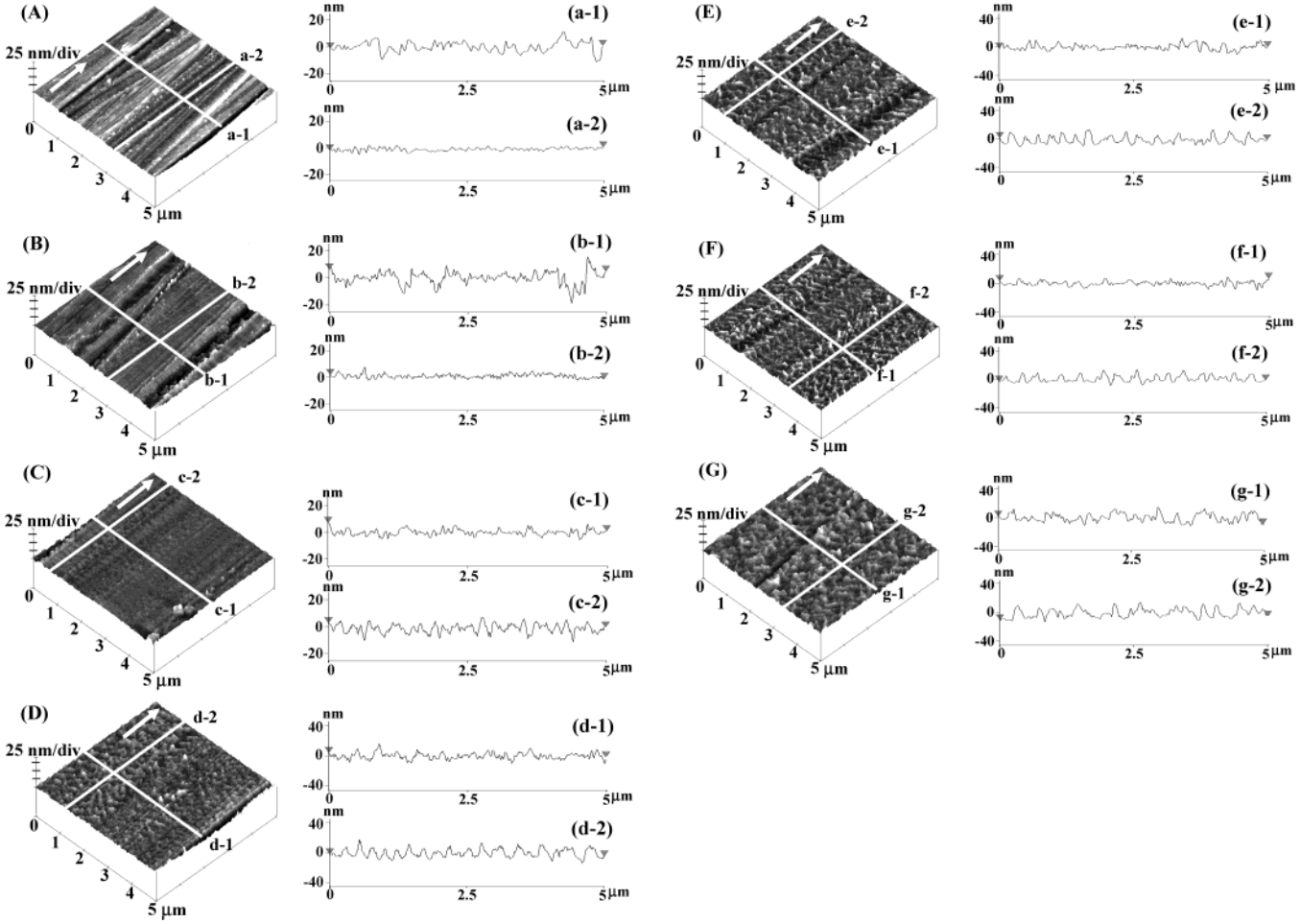

Figure 7. AFM images and surface profiles of PS films with various molecular weights rubbed with a rubbing density of 60: (A, a-1, a-2) 2700 $\overline{M}_w$; (B, b-1, b-2) 5200; (C, c-1, c-2) 9800; (D, d-1, d-2) 19 200; (E, e-1, e-2) 37 000; (F, f-1, f-2) 63 000; (g, G, g-1, g-2) 83 000.

rubbed film with 9800 $\overline{M}_w$, indicating that the meandering groovelike structures are better defined at this molecular weight.

Figure 7E−G shows AFM images of rubbed PS films of higher molecular weight (37 000−83 000 $\overline{M}_w$). As can be seen in these figures, the rubbed film surfaces of these higher molecular weight PS polymers are entirely covered by well-defined meandering groovelike structures. The rms surface roughness is 2.58−5.45 nm across the rubbing direction (Figure 7e-1,f-1,g-1) and 3.87−6.06 nm along the rubbing direction (Figure 7e-2,f-2,g-2).

The surface morphology of a rubbed PS film is clearly significantly dependent on the molecular weight. For PS films with $\overline{M}_w$ < 9800, submicroscale pebblelike grooves develop in the rubbed film surface along the rubbing direction. On the other hand, for PS films with $\overline{M}_w$ = 9800, submicroscale meandering groovelike structures are weakly developed in part along the rubbing direction, and their orientation directions lie perpendicular to the rubbing direction, in addition to the submicroscale pebblelike grooves as observed for the rubbed PS films with $\overline{M}_w$ < 9800. The meandering groovelike structures are well developed for PS films with $\overline{M}_w$ > 9800, covering the entire rubbed film surfaces. Rubbing of higher molecular weight PS films generates better defined meandering groovelike structures in the film surface. This topography is a significant departure from the previously reported surface topographies of rubbed PS films[7,8] and also from the surface morphologies observed for PI alignment layers.[3,4,7,10]

This variation in surface morphology might be due to the different deformation responses of the different molecular weight PS polymers to the shear forces caused by contact of fibers with the surface during the rubbing process. The deformation response of a PS film to these shear forces might be related to all the physical characteristics of the PS polymer chains. The first factor to consider is the polydispersity. All the PS samples used in this study have the same polydispersity (1.01−1.02) except for the slightly larger polydispersity (1.10) of the PS sample with 2700 $\overline{M}_w$, so the contribution of polydispersity to the deformation responses of the films should be constant. The second factor to consider is the chain rigidity. In general, PS is considered to have a flexible chain because of its relatively short Kuhn length [L_K(PS) = approximately 2 nm]; this parameter measures the rigidity of a polymer chain. Even though PS is a flexible polymer, its rigidity increases as its chain length decreases; in the extreme case, the PS chain is a rigid rod when its chain length is equivalent to its Kuhn length. Rigid polymer chains generally exhibit quite different viscosity and flow properties in the melt to those of flexible polymer chains. Thus, any variation in the chain length (i.e., molecular weight) of PS polymers is expected to be reflected in variation of the shear-induced deformations of films. The third factor to consider is the degree of chain entanglement. In

general, a shorter Kuhn length and longer chain length of a polymer results in a higher degree of chain entanglement. In the case of PS, the molecular weight (M_e) to occur chain entanglement is known to range from 17 300 to 18 100.[15] Thus, a PS film with higher molecular weight (>17 300 $\overline{M_w}$) has a higher degree of chain entanglement, which implies that more energy is required for shear-induced deformation. The fifth factor to consider is the chain mobility. The PS polymers in this study are amorphous, atactic polymers. As described above in the "Glass Transitions" section, a higher molecular weight PS sample exhibits a higher T_g; in particular, the T_g of PS is very sensitive to changes in the molecular weight for molecular weights of $\overline{M_w}$ < 19 200. Under a given set of conditions, a PS sample with a higher T_g has less chain mobility and thus is deformed more hardly by shear forces. We conclude that the parallel-oriented submicroscale groove morphologies observed on the rubbed films of low molecular weight PS polymers ($\overline{M_w} \leq 9800$) result from the lower energies of shear-induced deformation of these films, which are due to their shorter chain lengths, lower chain entanglements, and lower T_g, while the perpendicularly oriented submicroscale meandering groovelike structures observed on the rubbed films of high molecular weight PS polymers ($\overline{M_w} \geq 9800$) are due to the higher energies of shear-induced deformation of these films, which are due to their longer chain lengths, higher chain entanglements, and higher T_g.

A molecular weight dependency was also previously reported for the surface morphology of PS films multiline-scratched by using the silicon nitride and diamond tips of AFM;[16] in the scratching process the Hertzian contact pressure of AFM tips was very high (around 700 MPa), which far exceeds the critical Hertzian pressure value (around 96 MPa) of PS at which the plastic flow of PS occurs at the film surface, but the scratching speed was very low (around μm/s). The AFM-tip scratching of low molecular weight PS films (8000 $\overline{M_w}$) was found to generate a smooth surface topography, which is attributed to a plastic flow of the PS chains induced by contact of the mechanically hard, sharp AFM tip with the surface under the high loading pressure during the scratching process.[16] On the other hand, the AFM-tip scratching of high molecular weight PS films ($\overline{M_w} \geq$ 13 000) was found to generate a persistently periodic patterned structure perpendicular to the scratching direction, which is attributed to pulling (due to elastic nature of the PS surface) combined with stretching of the entanglement of the PS chains.[16] The formation of such patterned structure was enhanced with increasing $\overline{M_w}$ in the range of $\overline{M_w}$ < 58 000; for PS films with $\overline{M_w}$ ≥ 58 000, the enhancement of the patterned structure with varying $\overline{M_w}$ was not discernible.[16] The observation of these patterned structures indicate that the film surfaces of high-$\overline{M_w}$ PS behave more like a material exhibiting rubber elasticity than one in the glassy state.[16] These results collectively indicate that the transition between the smooth surface and the periodic patterned structure in the AFM-tip scratched PS film occurs around 13 000 $\overline{M_w}$. Because of the mechanically very high hardness of sharp AFM tips, the generation of smooth surface or patterned structure in the scratching of PS films was found to further depend on the scratching condition.[16,17] High contact pressure and rapid scan speed (e.g., ultrasonic scratch) in the scratch process tend to induce the plastic flow of PS chains rather than the viscoelastic deformation, consequently generating a smooth surface topography;[17] namely, higher contact pressure and more rapid scan speed cause to shift the PS molecular weight revealing the patterned structure toward the higher molecular weight region.

Taking these results into account, the perpendicularly oriented meandering groovelike structures observed on rubbed films of high-$\overline{M_w}$ PS might be attributed to pulling and scratching of the entanglements of PS chains (i.e., viscoelastic shear deformation of PS chains) during rubbing, which are dependent on the $\overline{M_w}$. Rubbing of even low-$\overline{M_w}$ PS films generated parallel-oriented pebblelike groove morphology rather than smooth surface. This fact indicates that although low-$\overline{M_w}$ PS films ($\overline{M_w} \leq 9800$) behave relatively weak resistance to the shear forces of the rubbing velvet fabric fibers in comparison to high-$\overline{M_w}$ PS films, in the rubbing process the low-$\overline{M_w}$ PS films undergo viscoelastic deformation or viscoelastic deformation combined with plastic deformation, rather than pure plastic deformation. This shear deformation of low-$\overline{M_w}$ PS films may be attributed in part from rayon fibers of the used velvet fabric, which are close to have the hardness of the PS films but much softer than the AFM tips used the scratching process.

In general, the shear deformation behavior of a polymer is known to significantly change below and above its entanglement molecular weight M_e.[15] Taking this fact into account, the transition of one surface morphology to another surface structure in rubbing of PS films is expected to occur at the M_e (= 17 300−18 100) of PS. However, the transition of the parallel-oriented pebblelike groove morphology to the perpendicularly oriented meandering groovelike structure in the rubbing of PS films occurs around 9800 $\overline{M_w}$, which is just approximately a half of the M_e. As described above, even in the AFM-tip scratched PS film the transition between the smooth surface and the periodic patterned structure also occurs around 13 000 $\overline{M_w}$, which is lower than the M_e. In fact, the M_e value known in the literature was estimated at the limit of zero shear rate for PS in the melt.[15] In contrast, the observed surface morphology changes have been measured for PS in the solid thin films that are rubbed with a rubbing speed of 480 mm/s, which is a high shear rate. Therefore, the discrepancy between the M_e and the $\overline{M_w}$ (for the transition of one surface morphology to another surface structure) might be attributed to the different states of PS samples as well as the different shear conditions.

In summary, the surface morphology of rubbed PS films is dependent on the velvet fabric characteristics (fiber diameter, structure of fiber end, fiber material, and fiber density of velvet fabric) and the rubbing condition [fiber depth (i.e., fiber contact pressure), rubbing roller speed, and rubbing table speed], in addition to the viscoelastic deformation characteristic of the PS films which is a function of molecular weight (i.e., chain length), molecular weight distribution, chain entanglement, and T_g.

LC Alignment. To examine the alignment behavior of LC molecules on the rubbed PS films with the surface morphologies shown in Figure 7, a solution of the Merck nematic LC in ethyl ether (10 wt % LC) was spin-coated onto the PS films, which were rubbed at a rubbing density of 60, as used in obtaining the AFM images in

Figure 7 and in the optical retardation measurements shown in Figure 3. For each LC-coated PS film, the transmitted light intensity was measured as a function of the angle of rotation of the film by using an optical retardation analyzer, and then a polar diagram of this variation was constructed. The measured light intensity is the product of the total "in-plane birefringence" and the total "phase" of the rubbed PS film and the coated LC layer. However, the in-plane birefringence of an aligned 300 nm thick LC layer is much larger than that of a rubbed PS film (the rubbed layer depth is typically less than 20 nm; see Figure 7) because the LC has very large anisotropic refractive indices ($n_e = 1.5697$ and $n_o = 1.4769$). The intensity variation and anisotropy of the polar diagram are mainly due to the coated LC layer. The polar diagrams are displayed in Figure 8.

Figure 8a shows a polar diagram of the transmitted light intensity for an LC-coated rubbed PS film with 2700 $\overline{M}_w$. In this figure, the maximum transmitted light intensity is along the direction 182° ↔ 2°, which is nearly parallel to the rubbing direction. This result indicates that the LC molecules in contact with the rubbed PS film surface are homogeneously induced to align nearly parallel to the rubbing direction.

Taking into account the surface morphology and reorientations of the polymer chain segments described above, these LC alignment data show that the LC molecules align parallel to the submicroscale grooves and the vinyl main chains (both oriented parallel to the rubbing direction), indicating that the alignment of LCs by PS films of this molecular weight is directly induced by the cooperation of the grooves and the reoriented vinyl main chains and not by the phenyl side groups, which are reoriented perpendicular to the rubbing direction.

This parallel LC alignment is a significant departure from the perpendicular LC alignments observed thus far for rubbed PS films.[5−7,9]

As can be seen in Figure 8b, the rubbed PS film with 5200 $\overline{M}_w$ aligns the LC molecules along the direction 160° ↔ 340°, which is separated by only 20° from the rubbing direction, i.e., the directions of the generated submicroscale grooves and the reoriented vinyl main chains, but is separated by 70° from the direction of the reoriented phenyl side groups. This result indicates that LC alignment on rubbed PS films of this molecular weight is also governed mainly by the cooperation of the grooves and the reoriented vinyl main chains (oriented parallel to the rubbing direction) and not by the phenyl side groups.

Unlike the rubbed PS films with 2700 and 5200 $\overline{M}_w$, the rubbed PS film with 9800 $\overline{M}_w$ aligns LCs in the direction 275° ↔ 95°, which is nearly perpendicular to the rubbing direction, as shown in Figure 8c. Taking into account the surface morphology and the reorientations of the polymer chain segments described above, this result indicates that on a rubbed film surface covered by both perpendicularly developed submicroscale meandering groovelike structures and by parallel developed submicroscale grooves, the alignment of LCs is induced mainly by the cooperation of the meandering groovelike structures and the phenyl side groups oriented perpendicular to the rubbing direction, not by the cooperation of the grooves and the vinyl main chains that are oriented parallel to the rubbing direction.

As can be seen in Figure 8d−g, the rubbed PS films (19 200−83 000 $\overline{M}_w$) that are covered by perpendicularly developed meandering groovelike structures align LCs in a direction perpendicular to the rubbing direction. These results indicate that the alignment of LCs is directly induced by the cooperation of the meandering groovelike structures and the phenyl side groups oriented perpendicular to the rubbing direction, not by the vinyl main chains oriented parallel to the rubbing direction.

Taking into account the lack of variation of the rubbing-induced reorientations of PS polymer segments with variation in the PS molecular weight, the above LC alignment data imply that the variations in the rubbed PS film surface morphology with molecular weight account for the variations in the alignment director of the LC molecules, which interact anisotropically with the submicroscale grooves and with the parallel reoriented vinyl main chains and the perpendicularly reoriented phenyl side groups.

LC Anchoring Energy and Alignment Stability. We prepared both antiparallel and TN LC cells and attempted to determine the polar and azimuthal LC anchoring energies and the LC alignment stability. Attempts to measure the polar LC anchoring energy in the antiparallel LC cells did not succeed because the LC alignments were completely destroyed even with very weak electric fields. However, we did succeed in measuring the azimuthal anchoring energy in the TN LC cells. The azimuthal anchoring energy measurements were only successful when carried out immediately after preparation of the TN cells because of the very limited stability of the LC alignment. Both the antiparallel LC cells and the azimuthal LC cells were found to have a stability of less than 1 day. The measured azimuthal LC anchoring energies ranged from 4×10^{-8} to 3×10^{-7} J/m^2, depending on the PS molecular weight; higher molecular weight PS films exhibited higher azimuthal energies, although all the measured azimuthal energy values are very small. In addition, for the antiparallel LC cells the LC pretilt angle was measured to be zero, regardless of the PS molecular weight; these results again confirmed the zero angle pretilt of LCs on rubbed PS films.[5,7,9]

The very low anchoring energy and the limited LC alignment stability suggest the following conclusions. First, LC molecules in contact with rubbed PS film surfaces interact only very weakly with the parallel reoriented vinyl main chains and with the perpendicularly reoriented phenyl side groups. Further, the strength of the interactions of the LCs with the reoriented vinyl main chains seems to be very close to that of the interactions of the LCs with the reoriented phenyl side groups. Second, the anisotropic interactions of the LCs with the submicroscale grooves in the rubbed film surface are also very weak. Of these three different anisotropic interactions between the LCs and the rubbed surface, none appears to dominate in determining the alignment of the LCs. Thus, when the anisotropic interactions of the grooves favorably cooperate with one of the other two anisotropic molecular interactions, they govern the alignment of the LC molecules.

In conclusion, the submicroscale grooves generated by rubbing PS films play a critical role in determining the alignment director of the LC molecules, which interact very weakly with the parallel reoriented vinyl main chains and the perpendicularly reoriented phenyl side groups.

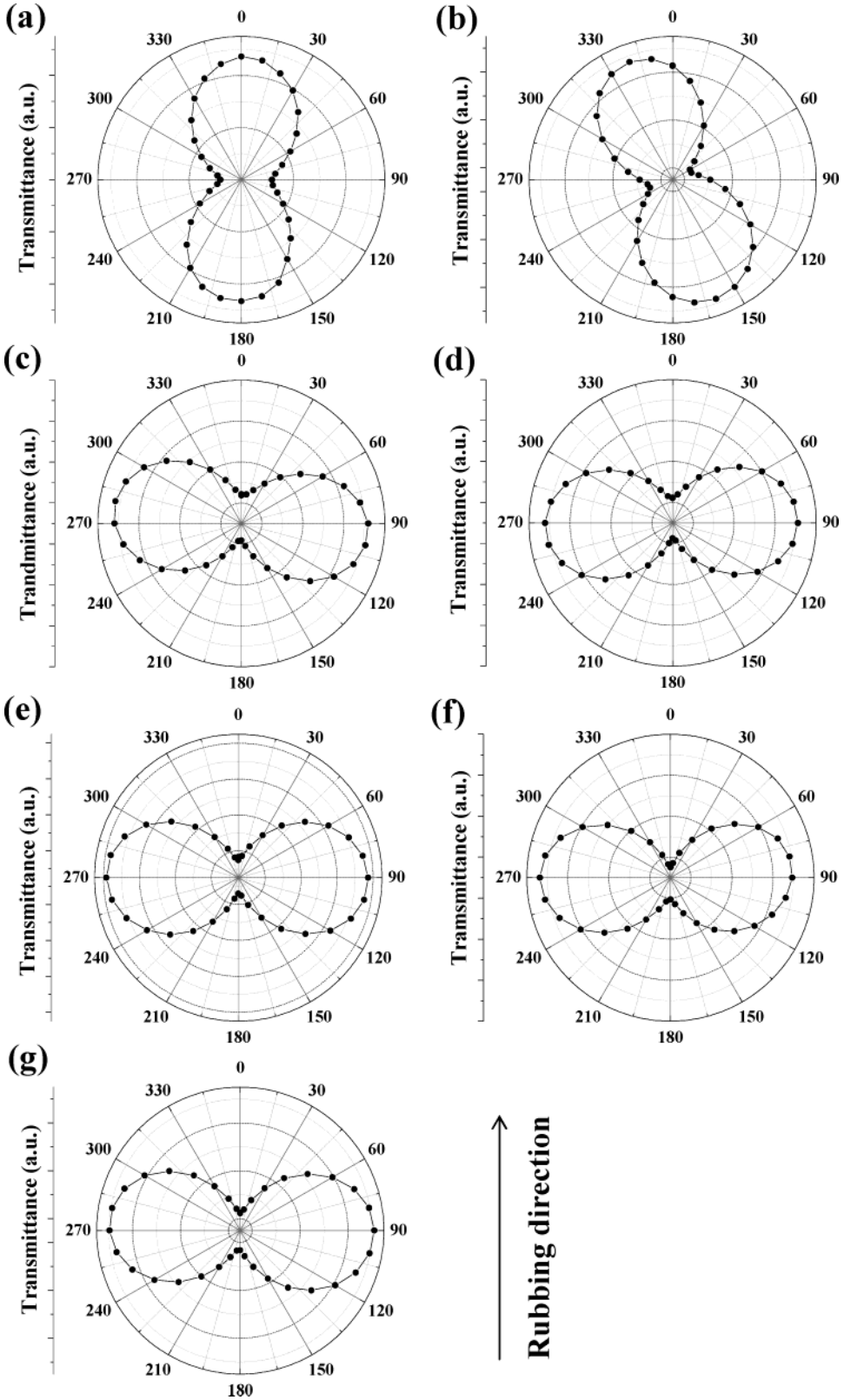

Figure 8. Polar diagram of the light transmittance [= (in-plane birefringence) × (phase)] taken from the optical phase retardation measurements of rubbed PS films with various molecular weights coated with a Merck nematic LC (MLK-6424: $n_e = 1.5697$ and $n_o = 1.4769$): (a) 2700 $\overline{M}_w$, (b) 5200, (c) 9800, (d) 19 200, (e) 37 000, (f) 63 000, and (g) 83 000. These PS films were all rubbed at a rubbing density of 60, and the thickness of the coated LC layer was 300 nm.

We recently discovered a polyimide (PI), poly{*p*-phenylene 3,6-bis[4-(*n*-butoxy)phenyloxy]pyromellitimide} (C4-PMDA-PDA PI, a well-defined brush PI composed of aromatic−aliphatic bristles set into a fully rodlike polymer backbone), that aligns LC molecules with a high anchoring energy in a direction perpendicular to the rubbing direction on the rubbed film surface, despite the reorientation of the polymer main chains along the rubbing direction and the development of submicroscale grooves along the rubbing direction.[10] We

concluded that the anisotropic molecular interactions of LCs with the reoriented C4-PMDA-PDA PI polymer segments are much stronger than the anisotropic interactions of the LCs with the submicroscale grooves. Further, the anisotropic molecular interactions of the perpendicularly reoriented phenyloxy side group units with LCs are stronger than those of the parallel reoriented polymer main chains with LCs, and this results in a LC alignment perpendicular to the rubbing direction.

From the results for rubbed PS and PI films, we propose the following general features of the alignment of LCs on rubbed polymer film surfaces: (i) the alignment of LCs with strong molecular interactions with the rubbed film surface is governed by the interactions with the reoriented main chain segments and side groups, all of whose directionally anisotropic interactions compete to align the LC molecules, with no significant contribution from the generated grooves, and (ii) the alignment of LCs with weak molecular interactions with the rubbed film surface is governed by the favorable cooperation of the interaction with the grooves with one of the interactions with the reoriented main chain segments and side groups, all of whose directionally anisotropic interactions compete to align the LC molecules.

Conclusion

The surface morphology and molecular reorientations of rubbed films of PS polymers with various molecular weights and narrow polydispersity were investigated in detail by AFM, optical retardation analysis, and linearly polarized IR spectroscopy. The alignments, pretilt angles, and anchoring energies of nematic LC molecules on the rubbed PS films were measured.

Rubbed PS films exhibit molecular reorientations that are independent of molecular weight: the vinyl main chains are preferentially reoriented along the rubbing direction while the planes of the phenyl side groups are reoriented perpendicular to the rubbing direction with para directions that are positioned nearly normal to the film plane.

However, the surface morphology of a rubbed PS film is significantly dependent on the molecular weight; submicroscale grooves develop along the rubbing direction in rubbed films of PS with $\overline{M_w} < 9800$, while for rubbed films of PS with $\overline{M_w} > 9800$, meandering groovelike structures develop perpendicular to the rubbing direction. The rubbing of higher molecular weight PS films generates better defined meandering groovelike structures in the film surface. These different surface morphologies might result from differences in the deformation responses of the different molecular weight PS polymers to the shear forces produced by contact of fibers with the surface during the rubbing process, which might originate in the variations in the physical characteristics (i.e., chain length, entanglement, glass transition temperature, etc.) of PS with molecular weight.

On these rubbed PS surfaces, LCs were found to anchor with a very low anchoring energy, ranging from 4×10^{-8} to 3×10^{-7} J/m^2, depending on the molecular weight, which results in limited stability (less than 1 day) of the LC alignment. The director of the LC alignment was found to always coincide with the orientation direction of the generated submicroscale grooves. This result suggests that the strength of the interactions of the LCs with the reoriented vinyl main chains seems to be very close to that of the interactions of the LCs with the reoriented phenyl side groups. Moreover, the anisotropic interactions of the LCs with the submicroscale grooves in the film surface are also very weak. Of these three different anisotropic interactions between the LCs and the rubbed surface, none seems to dominate in the determination of the alignment of the LCs. Therefore, the alignment of LCs with only weak molecular interactions with the rubbed PS film surface is governed by the favorable cooperation of the interaction with the submicroscale grooves (whose formation is strongly dependent on the molecular weight) with one of the interactions with the reoriented main chain segments and side groups, all of whose directionally anisotropic interactions compete to align the LC molecules.

Acknowledgment. This study was supported by the Korea Science & Engineering Foundation via the Center for Integrated Molecular Systems and by the Ministry of Education (BK21 Project).

References and Notes

(1) (a) Collings, P. J., Patel, J. S., Eds.; *Handbook of Liquid Crystal Research*; Oxford University Press: Oxford, 1997. (b) Cognard, J. *Alignment of Liquid Crystals and Their Mixtures*; Gorden & Breach: London, 1982.

(2) (a) Lee, K.-W.; Paek, S.-H.; Lien, A.; During, C.; Fukuro, H. *Macromolecules* **1996**, *29*, 8894. (b) van Aerle, N. A. J.; Tol, J. W. *Macromolecules* **1994**, *27*, 6520.

(3) (a) Kim, S. I.; Ree, M.; Shin, T. J.; Jung, J. C. *J. Polym. Sci., Part A: Polym. Chem.* **1999**, *37*, 2909. (b) Ree, M.; Kim, S. I.; Pyo, S. M.; Shin, T. J.; Park, H. K.; Jung, J. C. *Macromol. Symp.* **1999**, *142*, 73. (c) Ree, M.; Shin, T. J.; Lee, S. W. *Korea Polym. J.* **2001**, *9*, 1. (d) Park, J. H.; Sohn, B. H.; Jung, J. C.; Lee, S. W.; Ree, M. *J. Polym. Sci., Polym. Chem.* **2001**, *39*, 1800. (e) Lee, S. W.; Chae, B.; Lee, B.; Choi, W.; Kim, S. B.; Kim, S. I.; Park, S.-M.; Jung, J. C.; Lee, K. H.; Ree, M. *Chem. Mater.* **2003**, *15*, 3105.

(4) (a) Toney, M. F.; Russell, T. P.; Logan, J. A.; Kikuchi, H.; Sands, J. M.; Kumar, S. K. *Nature (London)* **1995**, *374*, 709. (b) Cossy-Favre, A.; Diaz, J.; Liu, Y.; Brown, H. R.; Samant, M. G.; Stohr, J.; Hanna, A. J.; Anders, S.; Russell, T. P. *Macromolecules* **1998**, *31*, 4957. (c) Mori, N.; Morimoto, M.; Nakamura, K. *Macromolecules* **1999**, *32*, 1488. (d) Weiss, K.; Woll, C.; Bohm, E.; Fiebranz, B.; Forstmann, G.; Peng, B.; Sheumann, V.; Johannsmann, D. *Macromolecules* **1998**, *31*, 1930. (e) Ge, J. J.; Li, C. Y.; Xue, G.; Mann, I. K.; Zhang, D.; Wang, S.-Y.; Harris, F. W.; Cheng, S. Z. D.; Hong, S.-C.; Zhuang, X.; Shen, Y. R. *J. Am. Chem. Soc.* **2001**, *123*, 5768. (f) Kim, Y. B.; Ban, B. S. *Liq. Cryst.* **1999**, *26*, 1579.

(5) Ishihara, S.; Wakemoto, H.; Nakazima, K.; Mastuo, Y. *Liq. Cryst.* **1989**, *4*, 669.

(6) Geary, J. M.; Goodby, J. W.; Kmetz, A. R.; Patel, J. S. *J. Appl. Phys.* **1987**, *62*, 4100.

(7) (a) Seo, D.-S.; Muroi, K.-I.; Isogami, T.-R.; Matsuda, H.; Kobayashi, S. *Jpn. J. Appl. Phys.* **1992**, *31*, 2165. (b) Seo, D.-S.; Oh-Ide, T.; Matsuda, H.; Isogami, T.-R.; Muroi, K.-I.; Yabe, Y.; Kobayashi, S. *Mol. Cryst. Liq. Cryst.* **1993**, *231*, 95. (c) Seo, D.-S.; Yoshida, N.; Kobayashi, S.; Nishikawa, M.; Yabe, Y. *Jpn. J. Appl. Phys.* **1995**, *34*, 4876.

(8) Wu, W. L.; Wallace, W. E. *J. Vac. Sci. Technol. B* **1998**, *16*, 1958.

(9) (a) Stohr, J.; Samant, M. G.; Cossy-Favre, A.; Diaz, Momoi, Y.; Odahara, S.; Nagata, T. *Macromolecules* **1998**, *31*, 1942. (b) Stöhr, J.; Samant, M. G. *J. Electron Spectrosc. Relat. Phenom.* **1999**, *98*−*99*, 189.

(10) Chae, B.; Kim, S. B.; Lee, S. W.; Kim, S. I.; Choi, W.; Lee, B.; Ree, M.; Lee, K. H.; Jung, J. C. *Macromolecules* **2002**, *35*, 10119.

(11) Sato, Y.; Sato, K.; Uchida, T. *Jpn. J. Appl. Phys.* **1992**, *31*, L579.

(12) (a) Yokoyama, H.; van Sprang, H. A. *J. Appl. Phys.* **1985**, *57*, 4520. (b) Nastishin, Yu. A.; Polak, R. D.; Shiyanovskii, S. V.; Bodnar, V. H.; Lavrentovich, O. D. *J. Appl. Phys.* **1999**, *86*, 4199.

(13) Yoon, K. H.; Ahn, S. H.; Kim, J. H.; Kim, W. Y.; Kwon, S. B. *Asia Display* **1998**, *98*, 1131.
(14) (a) Ren, Y.; Murakami, T.; Nishioka, T.; Nakashima, K.; Noda, I.; Ozaki, Y. *Macromolecules* **1999**, *32*, 6307. (b) Velada, J. L.; Cesteros, L. C.; Katime, I. *Appl. Spectrosc.* **1996**, *40*, 893. (c) Colthup, N. B.; Daly, L. H.; Wiberly, S. E. *Introduction to Infrared and Raman Spectroscopy*, 3rd ed.; Academic: San Diego, 1990.
(15) (a) Onogi, S.; Masuda, T.; Kitagawa, K. *Macromolecules* **1970**, *3*, 109. (b) Plazek, D. J.; Riande, E.; Markovitz, H.; Ragupathi, N. *J. Polym. Sci., Polym. Phys. Ed.* **1979**, *17*, 2189. (c) Ferry, J. D. *Viscoelastic Properties of Polymers*; John Wiley & Son: New York, 1980.
(16) (a) Meyers, G. F.; DeKoven, B. M.; Seitz, J. T. *Langmuir* **1992**, *8*, 2330. (b) Aoike, T.; Yamamoto, T.; Uehara, H.; Yamanobe, T.; Komoto, T. *Langmuir* **2001**, *17*, 5688. (c) Leung, O. M.; Goh, M. C. *Science* **1992**, *255*, 64.
(17) Iwata, F.; Matsumoto, T.; Ogawa, R.; Sasaki, A. *Jpn. J. Appl. Phys.* **1999**, *38*, 3936.

MA035258Z